

**PARTICLE REMOVAL IN POST CHEMICAL-MECHANICAL
PLANARIZATION (CMP) CLEANING PROCESS: EXPERIMENTAL AND
MODELING STUDIES**

Lok Yian Han

UNIVERSITI SAINS MALAYSIA

2009

**PARTICLE REMOVAL IN POST CHEMICAL-MECHANICAL
PLANARIZATION (CMP) CLEANING PROCESS: EXPERIMENTAL AND
MODELING STUDIES**

By

Lok Yian Han

**Thesis submitted in fulfillment of
the requirements for the degree of Master of Science**

JUNE 2009

ACKNOWLEDGEMENTS

First at all, I would like to express my deepest appreciation and gratitude to my supervisors Assoc. Prof. Dr. W.J.N Fernando, Assoc. Prof. Dr Mashitah Mat Don, Mr Venkatesh Madhavan and Mr Charlie Tay Wee Song of Silterra Sdn. Bhd.. Very much thanks for the infinite perseverance, enthusiasm and patient guidance. Secondly, I would like to thanks Mr Huang Kok Liang and Mr Dan Towery for their guidance and consultancy in this research.

Also many thanks are extended to the Universiti Sains Malaysia and Silterra Sdn. Bhd for giving me an opportunity to further my studies. My special acknowledgement goes to the Dean School of Chemical Engineering, Prof. Dr. Abdul Latif Ahmad for his support and help towards my Postgraduate work. Also not to forget to all staffs and technicians in School of Chemical Engineering and Silterra Sdn. Bhd for their co-operation and commitment.

My deepest gratitude goes to my beloved mother; Mrs. Law Siew Tee and In memory of my father Mr Lok Wai Seng for their endless love and support. Special thanks to my sister Mrs Lok Yian Yian and my brother in law Mr Lim Cia Ching for their valuable help during completion of my research.

To all my friends and colleague, Mr Chin Lip Han, Mr Lee Kang Hai, Miss Beryl Chua, Mr Lim Jew Tuang, Mr Edwin Goh, Mr Alex Quah, and others, thank you so much for your support and help.

Last but not the least; I would like to thank Mr Lum Sek Yew. Thank you so much for your motivation and unparalleled help. To those who indirectly contribute in this research, your kindness means a lot to me. Thank you very much.

Lok Yian Han, 2009

TABLE OF CONTENTS

	Page
ACKNOWLEDGEMENT	i
TABLE OF CONTENTS	ii
LIST OF TABLES	v
LIST OF FIGURES	vi
LIST OF ABBREVIATION	ix
NOTATIONS	x
ABSTRAK	xiv
ABSTRACT	xvi
CHAPTER ONE: INTRODUCTION	1
1.1 Introduction	1
1.2 Problem Statement	4
1.3 Research objectives	5
1.4 Organization of thesis	6
CHAPTER TWO: LITERATURE REVIEW	7
2.1 CMP Contamination	7
2.2 CMP Defect Classification	8
2.3 Post-CMP Cleaning	10
2.3.1 Scrubbing	11
2.3.2 Cleaning by Hydrodynamic jets	12
2.3.3 Megasonic acoustic cleaning	12
2.3.4 Cryogenic cleaning	13
2.3.5 Buffing	13
2.4 Force interactions in buffing	19
2.4.1 Particle attachment force	19
2.4.2 Particle detachment force	27
2.5 Particle removal mechanism	31
2.6 Statistical Analysis	36
2.7 Conclusions	39

CHAPTER THREE: MATERIALS AND RESEARCH METHODOLOGY	41
3.1 Materials	41
3.1.1 Test wafer, Polishing Pad and buffing pad	41
3.1.2 Slurries	42
3.1.3 Chemicals	42
3.2 Equipments	42
3.2.1 Chemical Mechanical Planarizer	42
3.2.2 Configuration of Cleaning System	44
3.2.3 SP1 KLA Tencor	45
3.2.4 SEM/EDS	45
3.3 Research Methodology	46
3.3.1 Preparation of test samples	46
3.3.2 Experiments	46
3.3.3 Statistical analysis	49
3.3.4 Determination of coefficient of friction (f)	51
3.4 Model Derivation	52
3.4.1 Theory	52
3.4.1.1 Adhesion force	52
3.4.1.2 Capillary adhesion force	54
3.4.1.3 Hydrodynamic force	55
3.4.1.4 Friction force and abrasion force	56
3.4.2 Forces Perpendicular to the buff pad	57
3.4.3 Resultant effect of Hydrodynamic Force and Friction Force	57
3.4.4 Criteria for Particle Removal	61
3.4.5 Evaluation of Particle Removal Efficiency	65
3.5 Overall Research Methodology Flow Chart	70
CHAPTER FOUR: RESULTS AND DISCUSSION	71
4.1 Introduction	71
4.2 Analysis of Particle Size Distribution in a Dirty Wafer	71
4.3 Experimental results	75

4.3.1	Dependence of particle removal efficiency to chemical flow rate	75
4.3.2	Dependence of particle removal efficiency to buffing disc pressure	79
4.3.3	Dependence of particle removal efficiency to relative buffing disc rotational speed	82
4.3.4	Overall Observations	85
4.4	Coefficient of Friction	85
4.5	Statistical Analysis	86
4.6	Mathematical Modeling	93
4.6.1	Hamaker Constant	93
4.6.2	Simulation of model	94
4.7	Discussion	99
CHAPTER FIVE: CONCLUSION AND RECOMMENDATION		102
5.1	Conclusion	102
5.2	Recommendation	104
REFERENCES		105
APPENDICES		110
A1	Explanation of infinitesimal area	110
A2	Derivation of b (center of gravity)	110
A3	Simulation steps by using Matlab	111
A4	Enlarge diagram for dirty wafer.	113
A5	Derivation of equation 3.37	114
A6	Example for the calculation of hamaker constant for citric acid	115
A7	Calculation of particle removal efficiency	116
LIST OF PUBLICATIONS&SEMINARS		118

LIST OF TABLES

Table 2.1	Typical Post CMP contamination	7
Table 2.2	Post CMP defects Classification	9
Table 2.3	The comparison of cleaning process	18
Table 3.1	Upper buff pad and lower platen rotational speed	44
Table 3.2	Parameters use for evaluate the particle removal efficiency	48
Table 3.3	Real and coded independent variables used in model	49
Table 3.4	Parameters use for evaluate the particle removal efficiency	50
Table 3.5	The chemicals properties used in this study	52
Table 4.1	Coefficient of friction for citric acid and de-ionized water as medium	85
Table 4.2	Analysis of variance (ANOVA) for the regression model equation of particle removal efficiency by using citric acid as the cleaning chemical	88
Table 4.3	Analysis of variance (ANOVA) for the regression model equation of particle removal efficiency by using de-ionized water as the cleaning chemical	89
Table 4.4	The estimated value of Hamaker Constant for de-ionized water and Citric acid	93

LIST OF FIGURES

Figure 1.1	Schematic of rotary CMP polisher	2
Figure 1.2	Schematic diagram for Polishing process of CMP	2
Figure 2.1	Example of wafer surface after scan with Laser scattering measurement instrument	8
Figure 2.2	Example of buffing system used in industry	14
Figure 2.3	Iron removal by different chemistries	15
Figure 2.4	The zeta potential of particles as a function of pH with and without the addition of citric acid	16
Figure 2.5	Interaction energy and force diagrams for particle surface interaction	20
Figure 2.6	Schematic representation of zeta potential	26
Figure 2.7	Diagram for friction force direction	24
Figure 2.8	Flow past immersed sphere	30
Figure 2.9	Forces applied on the wafer surface	31
Figure 2.10	Central composite design for three variables	38
Figure 3.1	Schematic diagram for Speedfam –IPEC Avantgaard 776 chemical mechanical planarizer	43
Figure 3.2	Configuration of cleaning system	45
Figure 3.3	Experimental setup for determined friction coefficient in different chemicals	51
Figure 3.4	Three dimensional diagram of the friction force and hydrodynamic force acting on the embedded particle	58
Figure 3.5	Schematic diagram for vector on buff pad and wafer	59
Figure 3.6	Force diagram for a particle embedded in wafer surface in the toppling plane	62
Figure 3.7	Force diagram for a particle embedded in wafer surface	63
Figure 3.8	Center of gravity for a particle embedded in a wafer	64

Figure 3.9	Flow chart showing modeling steps	66
Figure 3.10	Removal torque versus θ plot for different r_{wp}	68
Figure 3.11	Diagram for particle removal and unable to removal area	69
Figure 3.12	Research methodology flow chart	70
Figure 4.1	Typical Tencor scan of a test wafer	72
Figure 4.2	Plot of average probability of occurrence versus particle size distribution in a test wafer.	73
Figure 4.3	SEM scan for particle on wafer surface	74
Figure 4.4	The trace elements for particle observed on wafer surface.	74
Figure 4.5	Variation of particle removal efficiency vs. Citric acid flow rate for different relative buff rotational speed setting and different pressure settings.	76
Figure 4.6	Variation of particle removal efficiency vs. de-ionized water flow rate for different relative buff rotational speed setting and different pressure settings.	78
Figure 4.7	Plots of particle removal efficiency vs. buffing disc rotational speed for different citric acid flow rate and different buff rotational speed setting.	80
Figure 4.8	Plots of particle removal efficiency vs. buffing disc rotational speed for different de-ionized water flow rate and different buff rotational speed setting.	81
Figure 4.9	Particle removal efficiency vs. relative buff rotational speed setting for different citric acid flow rates at three different buffing disc pressures	83
Figure 4.10	Particle removal efficiency vs. relative buff rotational speed setting for different de-ionized water flow rates at three different buffing disc pressures.	84
Figure 4.11	Plot of experimental particle removal efficiency versus the predicted particle removal efficiency for citric acid.	87
Figure 4.12	Plot of experimental particle removal efficiency versus the predicted particle removal efficiency for de-ionized water.	89

Figure 4.13	The three dimensions plots of particle removal efficiency with respect of buffing disc pressure and chemical flow rate for different relative buff rotational speed setting (of 0,1,2) for Citric acid.	91
Figure 4.14	The three dimensions plots of particle removal efficiency with respect of buffing disc pressure and chemical flow rate for different relative buff rotational speed setting (of 0,1,2) for de-ionized water	92
Figure 4.15	Typical plots of Torque vs. θ for citric acid	96
Figure 4.16	Typical plots of Torque vs. θ for de-ionized water	97
Figure 4.17	Comparison of predicted model with experimental data for citric acid medium.	98
Figure 4.18	Comparison of predicted model with experimental data for de-ionized water medium	98

LIST OF ABBREVIATIONS

A1	Pad conditioner 1
A2	Pad conditioner 2
B1	Buff station 1
B2	Buff station 2
C	Cleaner
CCD	Central Composite Design
CMP	Chemical Mechanical Planarization
D1	Rinse station
D2	Brush stations
D3	Brush stations
D4	Spin rinse and dry channel
DOE	Design of experiment
DVLO	A theory present by Derjaguin, Landau, Verwey and Overbeek
EFF	Particle removal efficiency
ILD	Interlayer dielectric layer in wafer fabrication process
MP1	Polishing platen 1
MP2	Polishing platen 2
MP3	Polishing platen 3
MP4	Polishing platen 4
STI	shallow trench isolation layer in wafer fabrication process

NOTATIONS

Symbol	Description
A	Hamaker Constant
A_{11}	Hamaker constant of identical material 1 (J)
A_{12}	Hamaker constant between surface 1 and 2 (J)
A_{132}	Hamaker constant for material 1 and 2 in medium 3 (J)
A_p	Projected area of particle in the direction of flow (m^2)
a	Contact radius of particle with wafer surface(m)
B	Center of Buff pad
b	Distance of action of the drag force from wafer surface (m)
C_D	Drag coefficient
d_p	Diameter of the particle (m)
E	Young's modulus
F	Force (N)
\tilde{F}^*	Resultant force of hydrodynamic force and friction force (N)
F_A	Adhesion force (N)
F_{AA}	Adhesion force between particle and buff pad (N)
F_{CAP}	Capillary Force (N)
F_D	Hydrodynamic drag force (N)
F_{dl}	Double layer force (N)
F_R	Abrasion force in particle (N)
F_s	Shear stress (N)
f	Coefficient of friction

f_b	Factor of particle occupied area
G	Non-contact area from two parallel plate's area. (m^2)
\tilde{g}	unit vector perpendicular to the surface (inwards).
h	Particle-surface separation distance at contact (m)
K	Radius of the buff pad in the set up (m)
k	Boltzman constant
k'	Function of the ionic composition
l_2	Contact radius of the particle and wafer surface (m)
m	Molecular weight of the medium (g/mol)
M_1	The weight of the buff pad (g)
M_2	The total masses add to the string which is connect to buff pad (g)
M_R	Removal torque (Nm)
M_A	Attachment torque (Nm)
\tilde{m}	unit vector in the opposite of axial direction from particle along the buff pad
N	Avogadro number (mol^{-1})
\tilde{n}	Unit vector in the direction of abrasion
P	Pressure of buff pad to the particle (Psi)
P,E	Velocity of buff pad relative to earth (rpm)
P,W	Velocity of buff pad relative to wafer (rpm)
Q	Volumetric flow rate of chemicals (m^3/s)
\tilde{q}	unit vector in the direction of resultant force
r	Factor depending on the surface roughness
r_c	Radius of the contact line at the top of the meniscus. (m)

R	The radius of the sample wafer (m)
R_e	Reynolds Number
r_{wp}	Distance from location of particle to wafer center (m)
s'	Probability of removal of a particle
\bar{S}	Average probability of particle removal for all penetration depth
s''	Overall probability of particle removal
T	Temperature (deg. C)
u	Numerical of flow velocity of the stream passing the particle (m/s)
v	Relative velocity
\tilde{V}_{ab}	Abrasion velocity of the particle with the buff
ν'	Poisson ratio
ν_{perp}	Perpendicular component of the relative velocity
W	Center of wafer
W,E	Wafer rotational relative speed to earth (rpm)
x	The distance of particle location to buff pad center (m)
y_{max}	Factor depending on the surface roughness
Z_1	Buffing disc pressure
Z_2	Chemical flow rate
Z_3	Relative buffing disc rotational speed

Greek Letters

Symbol Description

ω_p	Upper buff pad angular velocity (rpm)
ω_s	Lower platen angular velocity (rpm)
ϖ	Thermodynamic work of adhesion (N)
γ	Surface tension (N/m)
ρ	Density of the chemical (kg/m ³)
α	Depth of the embedded particle below the surface (m)
μ	Fluid viscosity. (pa.s)
θ	Angle between BW and r_{wp} (deg)
ϕ	The maximum particle angle of θ when it is being polished (deg)
ψ	angle between line r_{wp} and extension of line x (deg)
δ	Particle toppling criteria
α	Relative approach between the particle and the surface (m)
η	Distance from location of particle to wafer center when Particle toppling criteria is meet. (m)
ε	Solvent permeability
ζ	Zeta potential
τ	Friction torque (Nm)

**PENYINGKIRAN BUTIR ZARAH BAGI PROSES PENCUCIAN
PASCA PERATAAN SECARA MEKANIKAL-KIMIA:
KAJIAN EKSPERIMEN DAN PEMODELAN.**

Abstrak

Proses pencucian pasca perataan secara mekanikal-kimia memainkan peranan penting dalam teknologi wafer kerana ia adalah salah satu objektif untuk menghasilkan permukaan yang berkualiti tinggi bagi dimensi yang halus. Kajian ini terdiri daripada eksperimen dan teori untuk menilai kecekapan penyingkiran zarah silikon dioksida (SiO_2) daripada permukaan wafer silikon semasa proses pencucian pasca perataan secara mekanikal-kimia (CMP). Kapasiti penyingkiran zarah daripada permukaan wafer melalui cakera pencucian dikaji menggunakan air dinyah ion dan asid sitrik dengan kadar pengaliran (dari 200 ml/min hingga 400 ml/min), tekanan cakera pencucian (1psi, 2psi dan 3psi), dan kelajuan cakera pencucian (0rpm, 1rpm and 2rpm) yang berbeza. Kecekapan penyingkiran zarah dalam setiap kes dikaji menggunakan jumlah zarah yang diukur melalui mesin pembiasan laser (SP1 KLA Tencor). Kecekapan penyingkiran zarah didapati meningkat dengan peningkatan kadar pengaliran, tekanan cakera pencucian dan kelajuan cakera pencucian.

Kaedah Permukaan Sambutan (RSM) telah digunakan untuk mengkaji kecekapan penyingkiran zarah bagi asid sitrik dan air dinyah ion melalui cakera pencucian. Kedua-dua asid sitrik dan air dinyah ion menunjukkan pekali kolerasi yang memuaskan dengan nilai pekali kolerasi ≥ 0.92 . Tekanan cakera pencucian dan kadar pengaliran kimia adalah ciri utama yang mempengaruhi penyingkiran zarah.

Satu model Matematik telah pun diterbitkan untuk mendapatkan korelasi kecekapan penyingkiran zarah dengan kadar pengaliran kimia, tekanan cakera

pencucian dan kelajuan relatif cakera. Dalam kes ini, daya individu yang bertindak ke atas zarah termasuklah daya geseran, daya pengusuran bendalir hidrodinamik, daya pelekatan dan daya kapilari juga turut dikaji. Suatu model teori telah diterbitkan dengan mengambilkira daya hasil dan momen pemutaran yang bertindak ke atas zarah terpancang dengan kedalaman yang berbeza. Simulasi telah dijalankan dengan mengguna model yang berasaskan pembolehubah-pembolehubah seperti ciri-ciri bendalir, geseran, dan parameter-parameter operasi (kadar pengaliran, tekanan dan kelajuan cakera.) Kecekapan penyingkiran zarah dalam simulasi telah dinilai dengan membandingkannya dengan data eksperimen. Data eksperimen dan model adalah bersesuaian dengan nilai pekali kolerasi 0.97 dan 0.85 untuk air dinyah ion dan asid sitrik.

**PARTICLE REMOVAL IN POST CHEMICAL-MECHANICAL
PLANARIZATION (CMP) CLEANING PROCESS:
EXPERIMENTAL AND MODELING STUDIES**

Abstract

The post chemical mechanical planarization (CMP) cleaning became very important in wafer technology as one of its objectives was to manufacture high quality surfaces of fine dimensions. This study comprises of an experimental as well as a theoretical study on particle removal efficiency mainly silicon dioxide (SiO_2) particles from wafer surface after chemical mechanical planarization (CMP) cleaning. The particle removal capacity from wafer surface in buffing (cleaning) disk was studied using de-ionized water and citric acid at different flow rates (200 ml/min to 400 ml/min) buffing disc pressure (1psi, 2psi and 3psi) and relative buffing disc speeds setting (0rpm, 1rpm and 2rpm). The removal efficiency in each case was evaluated using a particle count based on measurements with a laser scattering equipment (SP1 KLA Tenor). Particle removal efficiency was found to be increased with flow rates, buffing disc pressure and buffing disc speeds.

A Response Surface Methodology (RSM) couple with central composite design (CCD) was used in order to study the particle removal efficiency in the buffing disc for citric acid and de-ionized water. Both citric acid and de-ionized water showed satisfactory correlation with experimental value with correlation coefficient ≥ 0.92 . The significant factors affecting the particle removal efficiency were buffing disc pressure, relative buff rotational speed setting and chemical flow rate.

A mathematical model was also developed to correlate the particle removal efficiency in buffing disk with flow rate of chemical, buffing disc pressure and relative buffing disc rotational speed. In this case, the individual forces acting on a particle, namely frictional force, hydrodynamic fluid drag force, adhesion force and capillary force acting on a particle were analyzed. A theoretical model was developed taking into account the resultant forces on the particle and the toppling moments on a particle embedded in a wafer at varying depths. Simulations were also carried out using the model based on the physical variables such as fluid properties, frictional properties and operational parameters (flow rates, buff pressure and disc speeds). The evaluation of particle removal efficiency in this simulation was compared with experimental results. The experimental data and the model fitted well with a correlation coefficient of 0.97 and 0.85 for de-ionized water and citric acid, respectively.

CHAPTER ONE

INTRODUCTION

1.1 Introduction

In the semiconductor device fabrication, the various process steps fall into four general categories: deposition, removal, patterning and modification of electrical properties. As the device density on a chip increases, the metal interconnection density will increase. Thus, the interconnections occupy a large portion of the chip and they contribute to increasing interconnection related propagation delays. The solution to these problems is the use of a multilevel interconnection scheme where interconnections are made through vias in the different dielectric layers isolating various levels of interconnections. For such a scheme to work it is important that each level be flat so that patterning can be precise to allow vertical interconnections to be made.

There are several Planarization techniques have been used such as Chemical Mechanical Planarization (CMP), Doped glass reflow, hydrophobicity, spin etch planarization, spin on deposition, combination of ion etch with etch back, and combination of spin on deposition with etch back. CMP is the only technique achieves the greatest degree of planarization (Steigerwald *et. al.* 1997).

Chemical Mechanical Planarization (CMP) is a polishing process performed by the chemical reaction and mechanical action (Chen *et. al.* 2004). In a typical CMP machine, a wafer is mounted on a wafer carrier and is rubbed against a polishing pad under a load with a rotary motion in the presence of slurry (Zantyea *et al.* 2004). The schematic diagram of the Chemical Mechanical polisher is shown in Figure 1.1 and Figure 1.2 illustrated the process of CMP.

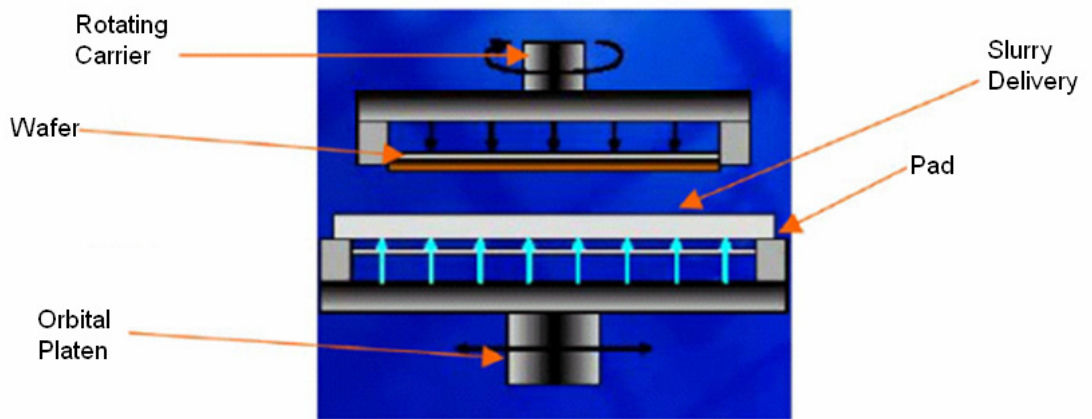


Figure 1.1: Schematic of rotary CMP polisher (Lee *et. al.* 2003).

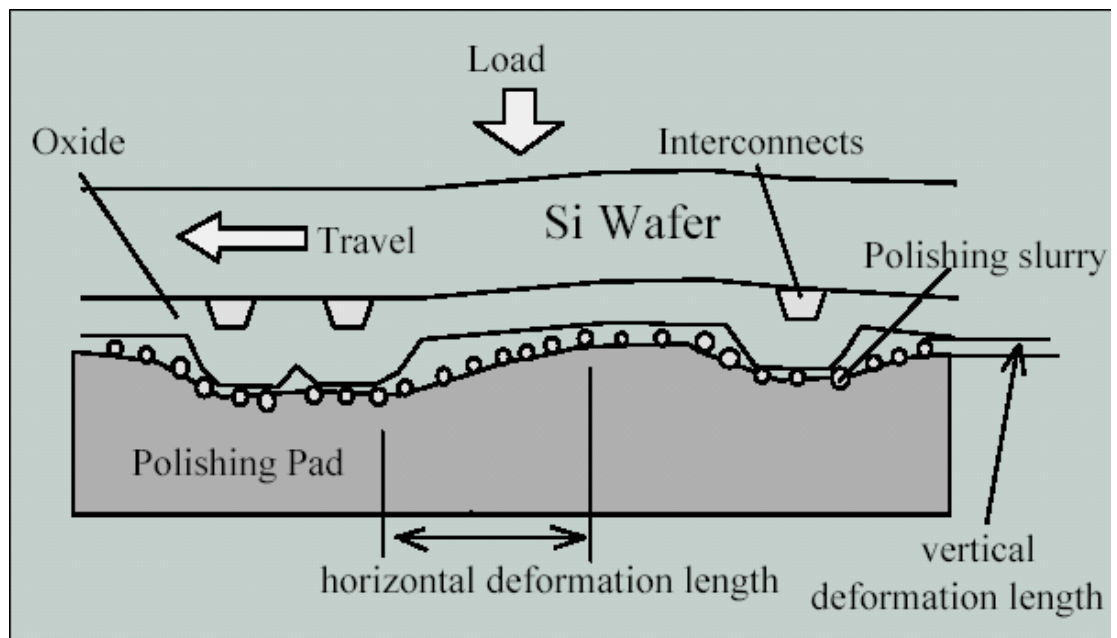


Figure 1.2: Schematic diagram for polishing process of CMP (Gutwein, 2005).

The slurry, usually contained a colloidal suspension of abrasive particles such as alumina and silica and special chemical additives and, was distributed throughout the pad and enhanced the chemical and mechanical action between the wafer and the pad. Polishing pad made of polymeric material (e.g. polyurethane) had porous surface where chemical reaction between the slurry and the wafer occurred.

This process involved intimate contact between the wafer surface and the pad material in the presence of slurry (Liu *et. al.* 1996), the debris from slurry will be left on the wafer surface after polishing as embedded particles (Zhang, 1999). The process for removal of this particle is termed as post CMP cleaning.

The post CMP cleaning became very important in wafer technology as one of its objectives was to manufacture high quality surfaces of fine dimensions (Zhang *et. al.* 1998). Procedures for the post-CMP cleaning process are developed and are already in use. A variety of procedures are available from which the most optimum, both performance wise and taking economical aspects into consideration are chosen based on the level of purity that is needed to be achieved and the amount of contamination that is expected out of the slurry composition and properties of the surfaces.

Typically post CMP cleaning is accomplished by methods such as wet chemical cleaning, buffing (Zhang, 1999), megasonic cleaning and brush scrubbing. In buffing, wafer is cleaned in soft buff pad under pressure in the presence of chemicals. In this process, it is expected that loose and embedded particle in the wafer are removed making the wafer surface a better quality product.

Previous researches have been found in trying to understand the mechanism of particle removal in post CMP cleaning. These include the basic cleaning principles (Zhang *et. al.* 1998), the effect of hydrodynamic force (Burdick *et. al.* 2003), modeling parameters to study the adhesion force (Liu *et. al.* 2003), study the lubrication behavior (Liang *et. al.* 2001) and friction force to different chemical during cleaning (Burdick *et. al.* 2005). Most of the study has been done to investigate single particle removal from wafer surface without considering the location of particle in wafer surface and the overall resultant effects of the forces. Thus, the

motivation of the model developed in this study is to predict the particle removal efficiency in different locations of the wafer for different particle diameter and penetration depth.

1.2 Problem Statement

Today's nano-scaled technologies of semiconductor wafer fabrication, wafer surface flatness and surface particle control become crucial as these parameters will determine the semiconductor device quality. Any defect left on wafer surface had lead to device function failure. Therefore, CMP and the cleaning process for particle removal after CMP are both the critical processes to ensure the quality of a wafer.

Silterra Sdn. Bhd. is a front-end semiconductor manufacturing for high technology investment in Malaysia. Messes Silterra have tried it manufacture wafer as output. CMP is one of the processes in wafer fabrication. Tungsten slurry has been used in the buff stations for post CMP cleaning. However, this chemical is an expensive chemical and contributes to high cost per wafer. There are also some unknown additives added in tungsten slurry had made the waste treatment of the used tungsten slurry become difficult. The untreated additives may bring the hazardous effect to the environment. Low cost chemical such as de-ionized water and citric acid have been selected by Messes Silterra to replace tungsten slurry in order to reduce the cost of ownership. The used de-ionized water and citric acid can also be well treat to reduce the hazardous materials released to environment.

Messes Silterra has engaged USM internship in the cleaning process after CMP to evaluate two types of buffing solutions for the cleaning process, namely de-ionized water and citric acid. Experimental evaluation for particle removal efficiency after CMP is required to enable implementation of both citric acid and de-ionized

water in mass production. However, the experimental evaluation of these solutions with different parameters required high end technology process. Hence, long term prediction of particle removal efficiency using a theoretical basis would prove to be useful. Further investigation on theoretical studies of particle removal in the process will allow a correlation between theoretical and experimental of particle removal efficiency.

1.3 Research objectives

In view of such a potential, this study was carried out with the following objectives:-

1. To evaluate particle removal efficiency from wafers in post CMP cleaning using an abrasion disk with de-ionized water and citric acid as cleaning solution.
2. To study the effect of chemical flow rate, rotational speed and buffing pressure to the Silicon Dioxide (SiO_2) particles removal efficiency from wafer surface.
3. To develop a theoretical and mathematical model that correlate the particle removal efficiency in an abrasion disk in term of frictional force, fluid drag, adhesion force and capillary force.
4. To compare the simulated data from the model with the experimental values.

1.4 Organization of Thesis

There are five chapters in this thesis including the current chapter. Each chapter gives important information of the thesis.

The next chapter presents the literature review. This chapter presents a review of literature on CMP defect, methods, chemicals used for post CMP cleaning, and model applicable to post CMP cleaning. Forces which contributed for particle attachment and detachment were also discussed in this chapter.

Chapter 3 covers the material and methods used throughout the current study. The first and second sections highlighted information about equipment and materials used in this study. The third section described about the experiment involved for cleaning. The last section describes the detail of mathematical model derivation and simulation.

Chapter 4 presents the experimental results together with the discussion. The first section described on particle removal efficiency using citric acid and de-ionized water as cleaning solution. Section two presents on the statistical analysis of the experiment results, followed by mathematical modeling and the evaluation between predicted and the experimental data.

Finally, Chapter 5 presents the conclusion and recommendations related to the study.

CHAPTER TWO

LITERATURE REVIEW

2.1 CMP Contamination

Since CMP involved the intimate contact of wafer surface with abrasion slurry and pad surface, wafer after CMP process is generally contaminated. The existence of particles contamination can be due to many other reasons such as suspended particles from various slurries (silica, alumina or ceria), from polished surface materials, from polishing pad and to an extent from the environmental conditions in which the process is taking place. However, in common CMP process, particle contamination was mainly due to residual particle generated from polishing pad and particles suspended in the slurry (Zantye *et. al.* 2004). The number of particles on the surface is specific to the process and type of slurry used for planarization. An example of contamination in CMP cleaning is shown in Table 2.1.

As shown in Table 2.1, the contamination for Interlayer dielectric (ILD) oxide CMP was silicon dioxide particle. Silicon dioxide was also the source of contamination for Tungsten CMP, shallow trench isolation (STI) oxide CMP and Copper CMP. Al_2O_3 and CeO_2 contaminant was usually contribute by the polishing slurry.

Table 2.1: Typical Post CMP contamination (Steigerwald, 1997).

CMP Process	Type of Particulate contaminant
ILD Oxide	SiO_2
Tungsten	Al_2O_3 and SiO_2
STI Oxide	CeO_2 and SiO_2
Copper	Al_2O_3 and SiO_2

2.2 CMP defects classification

CMP-related particles were typically measured on the front side of a wafer using laser-scattering instruments (Larious *et al.* 2003). Figure 2.1 showed the Example of wafer surface after scan with Laser scattering measurement instrument.

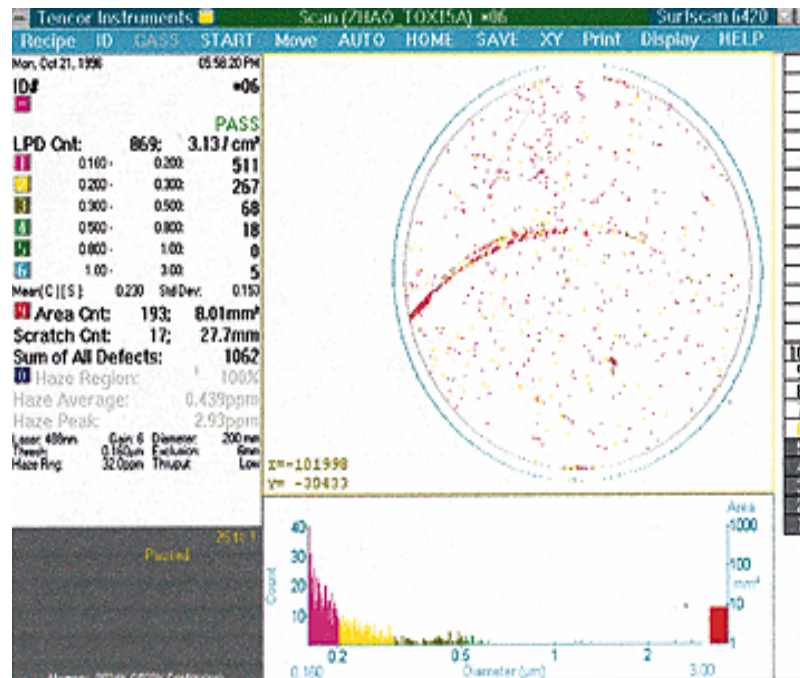


Figure 2.1: Example of wafer surface after scan with Laser scattering measurement instrument (Larious *et al.* 2003).

While this well-established technology offers reproducible and meaningful particle information, it has significant limitations (Larious *et al.* 2003). The main limitation of laser-scattering tools was that they cannot detect all particles based on their size, morphology, or location (Larious *et al.* 2003). For example, particles located in the edge-exclusion area or on the bevel edge of the wafer cannot be identified. There were classes of defects located on the front of a wafer that cannot be detected using particle counters because of size or morphological considerations. This type of contamination was easily visible with dark-field microscopy, scanning

electron microscopy (SEM), or atomic force microscopy (AFM), but it was difficult to quantify.

Larios *et.al.* (2003) classified the post oxide CMP defects as listed in Table 2.2. The metrology techniques suitable for identification of each defect classification and typical defect densities per wafer are also presented in the Table 2.2.

Table 2.2: Post CMP defects Classification (Larios *et. al.* 2003).

Class	Type	Typical Size	Metrology Technique	Preclean Defects/Wafer
A	Scratch	Few μm x several mm	Laser scattering	<5 counts
B	Area defect	0.5 μm x several μm	Laser scattering	20500 counts
C	Large particle	$\geq 0.1 \mu\text{m}$	Laser scattering	$>10^5$ counts
D	Small particle	$\leq 0.1 \mu\text{m}$	SEM, dark field, AFM	10^4 to 10^9 counts

The classes B, C and D as shown in the Table 2.2 were related to particle contamination. On a laser-scattering particle counter, Class B defect could appear as short area defects and may be misinterpreted as small scratches. However, under SEM or dark-field microscopy, many of these defects were clearly identified as slurry that appeared to be smeared across the wafer surface. This type of defect could be several microns wide and tens of microns long. The density of these defects was variable but seldom very large. The slurry that forms a Class B defect is strongly bonded to the wafer surface.

Class C defects were ubiquitous to CMP. These defects were slurry particles loosely attached to the wafer surface. These particles came in a range of sizes since they were caused by agglomeration of slurry particles. Class C defects were formed

from piles of individual slurry particles. SEM analysis has shown that these agglomerates were typically around 0.2 μm across and 0.1 μm to larger than 0.2 μm high.

Class D defects as listed in Table 2.2 were smaller than 0.1 μm . The density of these defects varied greatly, ranging from 10^3 to 10^9 defects/wafer. Class D defects were much smaller in size, could have an extremely high density with $>10^9$ per wafer, and could be difficult to remove. AFM and SEM analyses indicated that these defects were composed of a small number of individual slurry particles bound together. These slurry particles were seldom more than one layer thick, which accounted for their lack of height.

2.3 Post-CMP Cleaning

The presence of oxide residues after CMP has been one of the major issues in wafer technology. The colloidal debris from slurry left on the wafer surface after polishing contaminated the subsequent processing steps and caused functional defects and lowered the quality in the finished integrated circuits.

It has been found that it was practically impossible to clean the wafer surface if it dries before performing the cleanup unless the wafer surface is pre-conditioned immediately after the polishing step (Liu *et al.* 2003). Therefore chemical bonding of silica particles to the oxide surface occurred when it dehydrated. Once this occurred, the bonding was so strong that conventional chemical and mechanical cleanings of the surface become ineffective. Roy *et al.* (1995) showed that it has been common to use the wafer surface wet throughout the entire clean up process. In the polisher, the wafers were unloaded under de-ionized water stream and remain immersed in de-ionized water.

A variety of procedures for post CMP cleaning are available. General procedures used for post-CMP cleaning are given below:

- Scrubbing
- Cleaning by hydrodynamic jets
- Megasonic acoustic cleaning
- Cryogenic cleaning and
- Buffing

2.3.1 Scrubbing

Scrubbers and brushes were used for mechanically removing both the adhered as well as the mechanically embedded particles from the wafer surface. Brushes were used on single or both sides of the silicon wafer to scrub the surface thereby removing the particulates on the surface of the wafer. These brushes were typically made of polyvinyl alcohol (PVA) material, the texture of which was soft when wet. In spite of the name, it used hydrodynamic drag to exert a removal force on the surface particles. De-ionized water was typically used to generate electrostatic forces between the wafer surface and the dislodged particles to prevent the re-deposition of those particles. Zhang *et al.* (1998) carried out statistically designed experiments and stated that brush–wafer separation distance; brush down force (which was related to brush compression), brush rotation speed significantly affected particle removal during brush scrubbing. A relationship between brush compression and removal efficiency existed and indicated that hydrodynamic forces alone may not be responsible for particle removal during brush scrubbing. Zhang (1999) stated that higher pressure was more effective for slurry particle removal. This is because

higher pressure ensured the direct contact of brush and particles, thus providing much higher contact removal forces than non-contact hydrodynamic removal forces.

2.3.2 Cleaning by hydrodynamic jets

Cleaning by hydrodynamic jets basically involved impinging pressure jets on the wafer surface, which removed particles by hydrodynamic drag. There were low pressure and high-pressure hydrodynamic jets that were used for cleaning. Even though theoretically high-pressure jets were expected to remove particles more effectively, low-pressure jets were typically used to avoid damage to wafer surface. This process was more effective for small particles than micron size particles. This type of cleaning was found to be more effective than mechanical brush scrubbing in case of small particles (sub micron) (Li *et. al.* 2000). Furthermore, for micron size particles, the pressure to remove them was more than sufficient to damage patterned surfaces. Hydrodynamics played a major role in these types of mechanisms. Burdick *et. al.* (2001) had developed a numerical model, which described the effect of hydrodynamics on the particle removal. The model was developed based on the critical Reynolds number, which was independent of particle size. In some cases, spin-rinse drying was used, wherein the particle and chemicals on the surface were removed by centrifugal force along with the application of low-pressure sprays.

2.3.3 Megasonic acoustic cleaning

Ultrasonic and megasonic cleanings are an evolving technique for post-CMP cleaning process. This involved introducing frequency pressure waves in a cleaning bath using acoustic transducers. Megasonics was proven to be more effective than ultrasonic in sub micron range and it prevented defects like cavitations (Moumen *et*

al. 2004). In addition of the physical megasonic effect in removing the particles, the use of chemical has shown big improvements in cleaning efficiency. Megasonic cleaning efficiency depends on various parameters like power, length of cleaning and different temperatures.

2.3.4 Cryogenic cleaning

In cryogenic cleaning, liquid CO₂ at a high pressure was made to expand through a specially designed nozzle, in which the expansion of liquid CO₂ through the nozzle created solid and gaseous CO₂ in a highly directional and focused stream (Toscano *et. al.* 2002). There were three mechanisms by which surface cleaning was done: 1) momentum transfer by the cryogenic particles to overcome the force of adhesion of slurry particle to wafer surface, 2) drag force of gaseous CO₂ to remove the dislodged particle off the surface of the wafer, and 3) the dissolution of organic contaminants by liquid CO₂ formed at the interface of the cryogenic particle and wafer surface (Banerjee *e.t al.* 2008), (Lim *et.al.*2001)

2.3.5 Buffing

Many CMP technologies used multiple polishing steps to reduce particulate levels generated by the primary polishing step. For example, the first polish step on a hard pad was often followed with a de-ionized water (DI) buff on a soft pad as describe in Section 1.1. Most Common method of Post CMP cleaning was buffing using chemicals. An example of buffing system used in industry was shown as Figure 2.2.

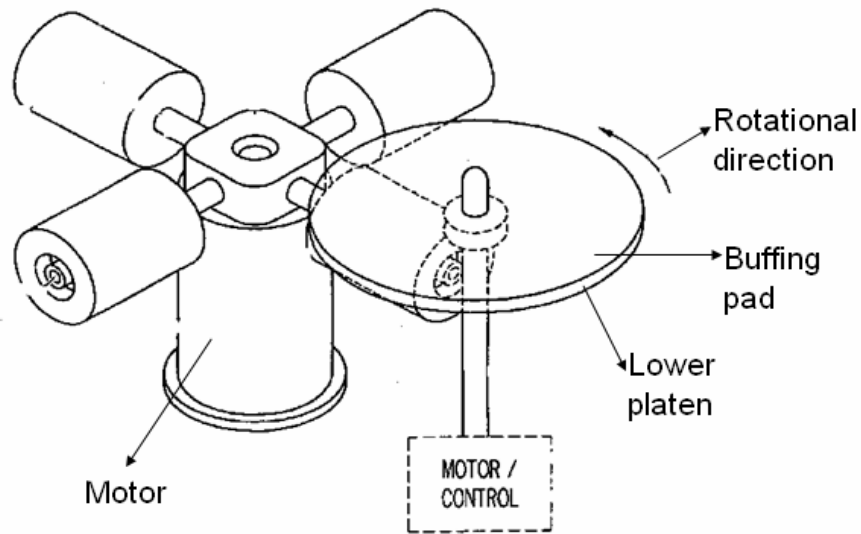


Figure 2.2: Example of buffing system used in industry (Bauer *et.al.* 2005)

Some defects, which were left out after polishing reside on the top layer of wafer. By buffing, defect was able to be removed in a shorter time (Larios *et. al.* 2003). Buley *et. al.* (2008) has demonstrated the used of chemical SP50A or SP28 as cleaning solutions in the buffing process, in conjunction with ESC784 cleaner, resulted in significantly lower defect counts.

Diluted hydrofluoric acid (DHF) has been used in buffing to remove contaminations left after polishing (Tardif *et. al.* 1997). It has been used in buffing to remove a thin oxide layer adhered and mechanically embedded particles (Roy *et. al.* 1995). Buffing using HF was reported to remove the defect and metallic contamination within 15 seconds (Wang *et. al.* 1998). It has been widely accepted that a dilute HF cleaning could provide a very low particle contamination.

Citric acid has been used in buffing to remove metallic contamination and organic residues from wafer surface (Park *et. al.* 2005). However, the study for the use of citric acid in particle removal was very limited.

Tardif *et. al.* (1997) in the research investigated the interaction among chemical and buff pad. In the research, pre-dirty wafer were buffed using different chemistry. Figure 2.3 shows that only citric acid present's sufficient iron particle removal efficiency. In the presence of citric acid, the adhesion force of the particle to wafer surface was reported to be lower than de-ionized water. (Park *et. al.* 2005). Thus the particle removal efficiency was higher as the adhesion force was lower. Buley *et. al.* (2008) has stated that citrate ion could remove the undercutting particles or organic defects in the wafer.

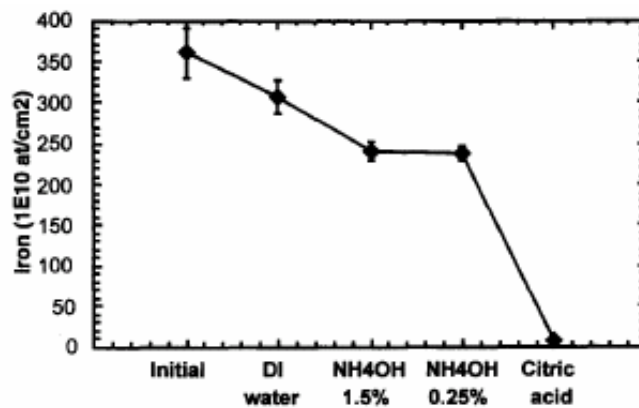


Figure 2.3: Iron removal by different chemistries. (Tardif *et. al.* 1997)

However, the use of citric acid could result in the same sign of zeta potential between wafer surface and particle. As the result, particle may reattach to the wafer surface. Usually a mechanical action (buffing) was required to avoid the particle reposition on wafer surface (Buley *et. al.* 2008). Figure 2.4 shows the zeta potential of particles as a function of pH with and without the addition of citric acid. The presence of citric acid results in slightly more negative zeta potential than values observed in silica particles at the same pH. (Park *et. al.* 2005).

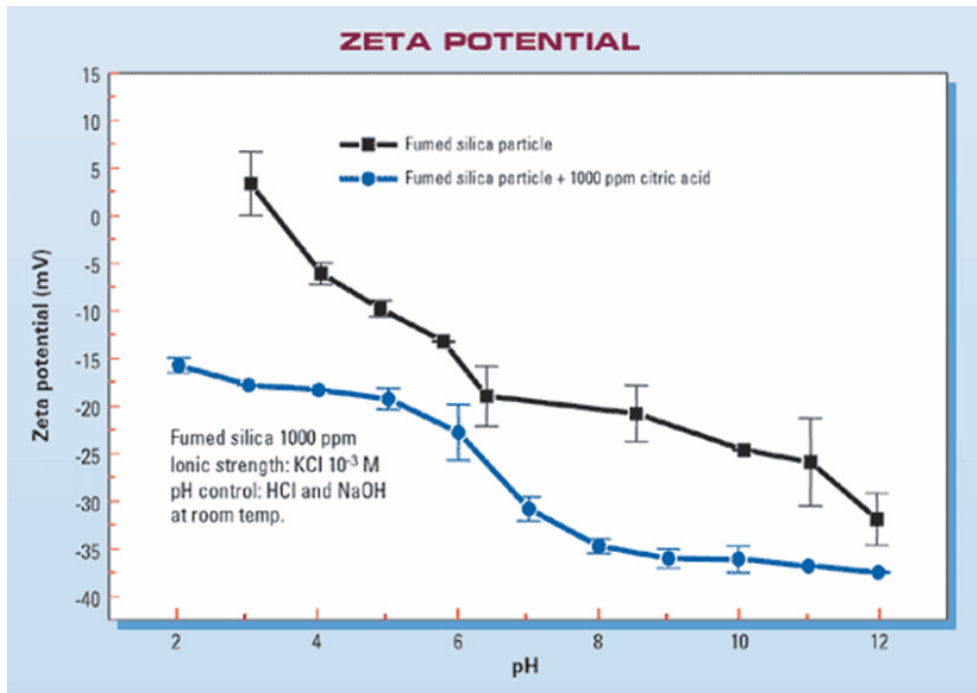


Figure 2.4: The zeta potential of particles as a function of pH with and without the addition of citric acid (Park *et. al.* 2005).

Ching *et al* (2003) proposed a post CMP cleaning using a buffer hydrofluoric (BHF) solution and ozone (O_3) treated water. The performance of the proposed cleaning technology has been investigated. The BHF solution was found to have the low level of contamination residues on the wafer surface. The high cleaning performance could be attributed to: (1) surface smoothing by surfactant in BHF solution, (2) etching effects of BHF, and (3) cleaning efficiency of O_3 water.

The use of surfactant as the cleaning solution was proposed by Liu *et. al.* (2003). It has been found that the non-ion surfactant molecules adsorbed preferentially onto the surface of the polished silicon wafer, and became a molecular layer with inner hydrophilic groups and outer hydrophobic groups. The outer molecular layer also adsorbed another reversed molecular layer, which formed the protective film on the surface of silicon wafer. The protective film prevents the formation of chemical adsorption and bonding between particle and silicon wafer.

Chen *et. al.* (2004) studied the buffing for colloidal silica abrasive removal from wafer surface. This process combined a buffing with dilute HNO₃/benzotriazole (BTA) aqueous solution and a polyvinyl alcohol (PVA) Triton X-100, for colloidal silica removal. It showed good colloidal silica removal ability by buffing with the HNO₃/BTA aqueous solution. After buffing, the wafer surface was basically hydrophobic, on which silica may re-adsorb. In order to remove residual colloidal silica completely, a PVA brush scrubbing process with Triton X-100 solution was introduced after buffing process. They have shown that a clean and smooth copper surface was obtained after this cleaning process.

Fisher and Misa (2005) claimed that cleaning by means of alkaline chemicals was desirable capable with CMP process which used alkaline slurries. By using an alkaline cleaning solution, the problem associated with swinging the pH in the process equipment can be avoided. The preferred cleaning agents include ammonium hydroxide and a tetra alkyl ammonium hydroxide. A cleaning solution embodiment contains tetra methyl ammonium hydroxide, ethylene diamine and a mixture of acetaminophenol and vanillin was suggested. A ratio of the concentrations suggested was in 2.75 wt% tetra methyl ammonium hydroxide, 6 wt% ethylene diamine, 0.75 wt% acetaminophenol and 1 wt% vanillin. For this embodiment, 15 times to 25 times dilution with deionized (DI) water should be made prior to use.

The buffing step, which was actually a mechanical cleaning step, produced a substantially cleaner surface. In buffing, besides the hydrodynamic forces exerting on particles, there were other forces arising due to the direct contact of the pad leading to removal of particles. Although high pressure was more effective for particle removal, a very high pressure on buff could cause the surface damage.

Chemicals used in buffing regulated the hydrodynamic force, capillary force; adhesion force and friction force surface tension which varied from one chemical to the other. In order to evaluate the performance of these chemical on buffing, it is necessary to understand the mechanism of removal and the forces theory. The following sections described these effects during planarization process.

2.3.6 Comparison of cleaning processes

The comparison of the cleaning process was shown in Table 2.3. Out of these cleaning processes, buffing was the most common used cleaning process.

Table 2.3: The comparison of cleaning process

Post CMP cleaning	Cleaning media	Particle removal concept	Advantages	Disadvantages	Reference
Scrubbing	Polyvinyl alcohol (PVA) brush	Hydrodynamic drag force Mechanical force	Good cleaning efficiency	Particle re-deposited on brush and cause further contamination Scratches	Zhang <i>et al.</i> (1998)
Hydrodynamic jets	Pressure jets	Hydrodynamic drag force	Low cost and easy maintenance	High pressure will cause the structure damage	Li <i>et al.</i> 2000
Megasonic acoustic	Frequency pressure wave by acoustic transducer	Megasonic power	Good cleaning efficiency	High cost process Risk of structural damage	Moumen <i>et al.</i> 2004
Cryogenic cleaning	High pressure liquid carbon dioxide	Hydrodynamic drag force	Good cleaning efficiency Organic contamination can be removed.	High cost Risk of structural damage	Toscano <i>et al.</i> 2002
Buffing	Buff pad	Hydrodynamic drag force Mechanical force	Good cleaning efficiency	Scratches	Park <i>et al.</i> 2005

2.4 Force interactions in buffing

A particle on a wafer surface which undergone buffing, produced many forces such as frictional force on the buff, hydrodynamic force, adhesion force, capillary force and electrostatic force.

2.4.1 Particle attachment forces

Adhesion force

When the surfaces of two solid materials approach at distances of the order of atomic dimensions (around ten to hundreds of angstroms), an attractive force was exerted between the surfaces. This force was associated with the Van der Waals or London force between atoms of the solids (Middleman *et.al.* 1993; Paajanen. 2006). These forces were diminished as the surface approach to within even smaller distances (ten of angstroms or smaller) until ultimately a repulsive force was exerted. An interaction energy diagram and the corresponding force diagram are shown schematically in Figure 2.5.

The first minimum in the interaction energy diagram corresponding to a separation distance at which the attractive and repulsive forces balanced. A pair of surfaces at this separation would appeared to be bound together; in the sense that the position was stable and a force would be required to separate them further. The distance h is called the adhesion distance (or particle-surface separation distance) and the force is the force of adhesion (Middleman *et. al.* 1993).

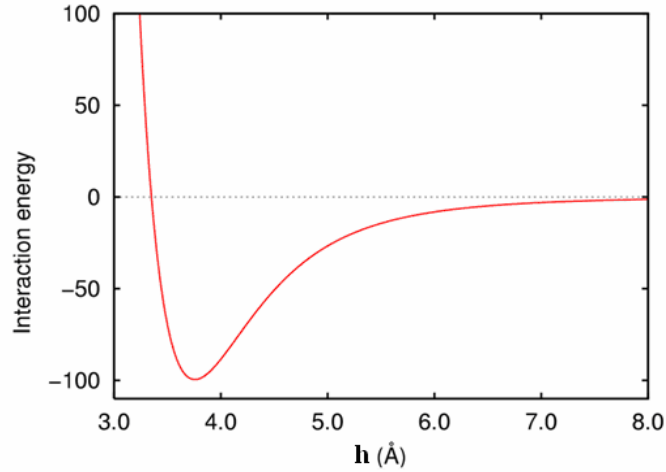


Figure 2.5: Interaction energy and force diagrams for particle surface interaction (Middleman *et. al.* 1993).

At these distances, the particles were bound to the surface by Van der Waals attraction. Other forces, such as electrostatic double layer force, also contributed to the net force between the particle and the surface but the Van der Waals force was universal and dominating (Donovan, 1990; Eichenlaub *et. al.* 2006).

Over the last century, a number of theories have been proposed to quantify the interfacial Van der Waals forces. The London-Van der Waals attractive force at solid interfaces that occurred as a result of fluctuating dipoles at the atomic level was integrated by Hamaker (Middleman and Hochberg, 1993) to predict the attraction between two macroscopic non-deformable bodies. The Van der Waals force based on Hamaker integration can be expressed as

$$F = \frac{Ad_p}{12h^2} \quad (2.1)$$

where

d_p = Particle diameter

A = Hamaker Constant

h = Particle-substrate separation distance

The Hamaker integration predicted the adhesion force by assuming that both of the surfaces were smooth. However, a majority group of materials have rough surfaces. Rabinovich (2000) has modified the Hamaker integration to account the surface roughness effect to the adhesion force. The Rabinovich theory was shown as in equation (2.2). However, the Rabinovich theory was reported to over estimate the adhesion theory (Li et. al. 2006).

$$F = \frac{Ad_p}{6h^2} \left(\frac{r}{r+d_p} + \frac{1}{\left(1 + \frac{y_{\max}}{h}\right)^2} \right) \quad (2.2)$$

where y_{\max} and r were factors depending on the roughness

Katainen *et. al.* (2006) modified Rabinovich theory and derived a new model which took into account multiple contacts with the surface by assuming number of possible contact points for flat particle and evaluated an equation for the adhesion forces given in equation (2.3).

$$F_A = \frac{AG}{6h^2} \left(\rho_a r + \frac{1}{\pi h \left(1 + \frac{y_{\max}}{h}\right)^3} \right) \quad (2.3)$$

where

G = Non-contact area from two parallel plate's area.

ρ_a =Density of asperities.

Their findings have shown that the relative size of the adhering particles and the surface properties such as roughness played an important role in the interaction. The model derived has been reported to be in agreement with their experiment results.

Derjaguin *et al.* (1975) proposed a theory which was reported to be applicable for two small, hard solid particles with low surface energy. According to the model, the pull-off force was expressed as:

$$F = 4\pi d\gamma \quad (2.4)$$

The contact area was defined as

$$a = \sqrt[3]{3\pi\gamma d_p^2 (1 - \nu'^2) / E} \quad (2.5)$$

where

γ = Surface energy of the sphere

ν' = Poisson ratio

E = Young's modulus

This model was referred to as the DMT model. The DMT model treated the condition such that two spheres were in intimate contact. The application of DNT model was only limited to the spheres with smooth surface.

Li *et al.* (2006) combined DMT model and the Rumpf model (1990) to obtain:

$$F = 4r\ell\pi + \frac{A}{6} \left(\frac{d_p}{(h+r)^2} \right) \quad (2.6)$$

As a result, Li model is reported to have a higher magnitude of adhesion force. The second term of the model seemed to be negligible in most practical cases where the main bodies were often separated by more than 20 nm. When the asperities (surface roughness) were smaller than 20 nm, the mathematical expression of adhesiveness took a different form with consideration of the main body.

For small, spherical particles in contact with a smooth surface in de-ionize water medium, an equation has been presented as (Burdick *et al.* 2003):-

$$F_A = \frac{A_{132}d_p}{12h^2} \left(1 + \frac{2a^2}{hd} \right) \quad (2.7)$$

where

F_A = Adhesion force (N)

h = Particle-surface separation distance at contact (m)

a = Contact radius of particle with wafer surface (m)

Notation A_{11} was used to refer to the Hamaker constant between like surfaces. For the interaction between two dissimilar surfaces, notation A_{12} was used. If the two surfaces were separated by medium, notation A_{132} was used where subscript 3 referring to the medium. For a pair of dissimilar bodies, the Hamaker constant A_{12} was related to the individual constant A_{11} and A_{22} for bodies 1 and 2 as (Middleman and Hochberg, 1993):-

$$A_{12} = (A_{11}A_{22})^{1/2} \quad (2.8)$$

When an intervening medium is significant, the appropriate constant to use is

$$A_{132} = A_{12} + A_{33} - A_{13} - A_{23} \quad (2.9)$$

Equation 2.7 has been modified to take into account the effect of roughness on the Van der Waals forces. This approach incorporated the Hamaker constant, A , an assumed separation distance at contact $h=0.4$ nm. The model derived has been reported to be in good agreement with their experiment results (Burdick *et. al.* 2003; Burdick *et. al.* 2005).

Capillary force

The effect of capillary is important just as adhesion force in buffing mechanism. In many cases, more simplistic approaches can be successful but for nano scale particle, simplistic capillary force model may be invalid. The force due to

capillary pressure on a particle can be expressed as in equation (2.10). This equation was derived by the assumption that the particle size is a sphere and the meniscus followed the sphere shape (Pakarinen *et.al.* 2005):

$$F_{CAP} = \pi r_c^2 \frac{kT \ln\left(\frac{P}{P_s}\right)}{m} \quad (2.10)$$

where

m =Molecular volume of the liquid.

k = Boltzman constant

T = Temperature.

$\frac{P}{P_s}$ =Relative humidity

r_c = Radius of the contact line at the top of the meniscus.

For a particle in wafer that was exposed to a fluid, the capillary adhesion force became significant. The force of capillary adhesion given by Donovan *et. al.* (1993) and Pakarinen *et. al.* (2005) can be expressed as

$$F_{CAP} = 2\pi d_p \gamma \quad (2.11)$$

For a particle on a smooth surface, this equation is satisfactory.

Electrostatic Forces

A theory presented by Derjaguin, Verwey, Landau, and Overbeek (Malvern Instruments, 2009) commonly name as DVLO theory suggested that the stability of a particle in solution was dependent upon its total potential energy V_T . This theory recognized that V_T was the balance of several contributions:

$$V_T = V_A + V_R + V_s \quad (2.12)$$